A generic model for MIMO wireless propagation channels

Andreas F. Molisch, *Senior Member, IEEE*

***Abstract*— We study the MIMO wireless channel, and derive a generic channel model that we believe has the ability to explain all important effects, including (i) interdependency of directions-of-arrival and directions-of-departure, (ii) large delay and angle dispersion by propagation via far clusters, (iii) rank reduction of the transfer function matrix. We point out the relevant propagation effects, and propose a geometry-based model that includes the relevant effects. The required parameters for the complete definition of the model are enumerated, and typical simulation results for urban macrocells are presented.**

***Index Terms*— MIMO, channel model, keyholes, dispersion**

I. Introduction

In the last years, MIMO (multiple-input - multiple-output) systems have emerged as one of the most promising approaches for high-datarate wireless systems [1], [2]. With the growing importance of MIMO systems, there is an increasing need for appropriate channel models. These channel models require two steps: (i) setting up a generic channel model and identifying the parameters that have to be determined for a full description and (ii) actually performing the measurement campaigns, and extracting the parameters. At the moment, there are not many MIMO measurement campaign results available publicly, but this is going to change in the next years. In order to allow best benefits from those campaigns, the first step, namely the setting up of a generic channel model, is urgently required.

For the standard narrowband channels, the generic model consists of an attenuator with a prescribed Doppler spectrum (time variance of the attenuation). In the wideband case, a tapped-delay line (with possibly different) Doppler spectra for each tap has been proposed in the 1960s. The much more involved generic framework of the "single-directional channel", either based on a geometric or a purely stochastic approach, was established in the mid- and late 1990s [3]. All those generic models are now well-established, even though we note that the actual *values* of the parameters are still subject to discussion for different environments[1].

There are also some MIMO channel models available in the literature, but they are essentially constructions suited to specifically reproduce a certain effect. The most simple, and still most widely used, model is the independent Rayleigh fading at all antenna elements, introduced in [1] and also used in [2]. Subsequently, [4] has analyzed the effect of correlation. It used a geometrically- based stochastic approach, placing scatterers in a random around the MS - a model that dates back to the early 70s [5], [6]. The implications of a more general, cluster-based model introduced in [7] were analyzed by [8]. All those models were based on the assumption that only single-scattering processes occurred, or that at least all those processes could be represented adequately by "equivalent" single-scattering processes. However, the analysis of a group from Stanford [9] and one from Bell-Labs [10] showed the occurrence of so-called "keyhole-" or "pinhole-" channels whose behavior could not be explained adequately in terms of single scattering. To wit, low-rank channel transfer matrices are possible even when the entries into those matrices are uncorrelated. [9] also gave a channel model that could explain the behavior by decomposing the channel correlation matrix into three terms. The thesis [11] investigated the influence of polarization.

None of the above models is general enough to incorporate all channel-induced effects relevant for MIMO systems. In this paper, we develop a model that remedies the situation. Our new model is based on a geometric approach, combined with physical arguments about the relevant propagation effects. In section II, we discuss the different propagation effects and point out their most important properties. Section III outlines the model structure, and enumerate all variables that are necessary to fully parametrize the model, and gives some typical simulation results. A summary concludes this paper.

II. Channel description methods and propagation processes

A. Vector versus double-directional representation

MIMO channels can be modeled either as double-directional channels [12] or as vector (matrix) channels [2]. The former method is more related to the physical propagation effects, while the latter is more centered on the effect of the channel on the system. Still, they must be equivalent, as they describe the same physical channel. Another distinction is whether to treat the channel deterministically or stochastically. In the following, we outline the relations between those description methods.

From the *deterministic* point of view, the *double-directional channel* can be modeled in a rather straightforward way: we need to investigate the double-directional impulse response. It

The author is with the Wireless Systems Research Department, AT&T Labs - Research, 200 Laurel Av., Middeltown, NJ, USA. E-mail: afm@research.att.com.

[1] Even though much progress has been made, especially in the context of the European COST actions, some radio environments are still essentially open problems.

0-7803-7400-2/02/$17.00 © 2002 IEEE

includes all N resolvable propagation paths between the transmitter and the receiver sites. Each path is delayed in accordance to its excess-delay τ_i, weighted with the proper complex amplitude $a_i e^{j\phi_i}$, and each direction-of-departure (DOD) $\Omega_{T,i}$ is connected to the corresponding direction-of-arrival (DOA) $\Omega_{R,i}$,[2]

$$h(\tau, \Omega_R, \Omega_T) = \sum_{i=1}^{N} h(\tau_i, \Omega_{R,i}, \Omega_{T,i}) \quad (1)$$

$$= \sum_{i=1}^{N} a_i e^{j\phi_i} \delta(\tau - \tau_i) \cdot \ \delta(\Omega_R - \Omega_{R,i}) \ \delta(\Omega_T - \Omega_{T,i}).$$

In general, all multipath parameters in (1), $\tau_i, \Omega_{R,i}, \Omega_{T,i}, a_i e^{j\phi_i}$ will also depend on the absolute time t. Then, also the set of multipath components (MPCs) contributing to the propagation will vary, $N \rightarrow N(t)$.

The *deterministic* wideband *matrix* channel response can be computed for any antenna constellation as

$$h(\tau, x_R, x_T) = \sum_{i=1}^{N} h(\tau_i, \Omega_{R,i}, \Omega_{T,i}) \cdot \quad (2)$$

$$\cdot g_R(\Omega_R) g_T(\Omega_T) \cdot \ e^{j\left\langle \vec{k}(\varphi_{R,i}) \vec{x}_R \right\rangle} e^{j\left\langle \vec{k}(\varphi_{T,i}) \vec{x}_T \right\rangle},$$

where $\vec{x}_R$ and $\vec{x}_T$ are the vectors of the chosen element-position measured from an arbitrary but fixed reference point on the corresponding array, and

$$\left\langle \vec{k}(\Omega) \cdot \vec{x} \right\rangle = \frac{2\pi}{\lambda} (x \cos\vartheta \cos\varphi + y \cos\vartheta \sin\varphi + z \sin\vartheta). \quad (3)$$

where ϑ and φ denote elevation and azimuth, respectively.

The above *double-directional* description seems rather straightforward. However, a straightforward *stochastic* description of the involved parameters involves a four-dimensional power spectrum that could only be described or saved as a huge file. Note that in general, the statistics of MPC delays, DOAs, DODs, amplitudes and phases are not separable, and thus have to be described by their joint probability density function. As we will see later on, even the common assumptions of Rayleigh-distrtibuted amplitudes and uniformly distributed phases are too restrictive, as they cannot reproduce the important "keyhole" effect.

The *stochastic* description of the *matrix channe*l also seems simple at first glance. It requires the average powers of the entries of the transfer matrix (from each transmit to each receive antenna), as well as the correlation between the matrix entries. Especially for small antenna array sizes, a description of the H-matrix seems desirable. However, we have to keep the following point in mind:

[2]We stress that the (double-directional) channel is reciprocal. While the directions of multipath components at the base station and at the mobile station are different, the directions at one link end for the transmit case and the receive case must be identical. When we talk in the following about DOAs and DODs, we refer to the directions at two different link ends.

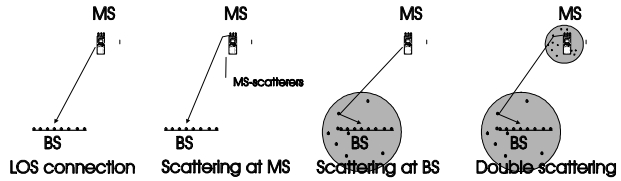

Fig. 1. Scattering around BS and MS.

1) the fading at the different antenna elements can be Rayleigh, Rician, or "double-Rayleigh" (as we will see below). Thus, we have to define those statistics and its associated parameters.
2) the number of involved correlation coefficients increases quadratically with the number of antenna elements. Their number might be reduced in periodic structures, as can be usually found at base stations (BSs) (Toeplitz structure of the correlation matrix for antenna arrays), but not necessarily for diversity arrangements as found at the mobile station (MS).
3) the whole description becomes dependent on the used antenna arrangement. Generalizations to larger (or just different) structures are not easily possible.
4) in delay-dispersive environments, we have to define different correlation factors for each delay - different propagation mechanisms (which induce different correlation factors) have different delays.

In order to avoid these problems, it is necessary to come up with a new model that allows some simplifications, but is still general enough to include clustering, waveguiding, etc. In the following, we will develop such a model. It is based on the GSCM (geometry-based stochastic channel model) of Fuhl, Molisch, and Bonek [7], but with several modifications that allow MIMO-specific effects to be included. Since the model is geometry-based, and thus emulates physical propagation processes, we first have to determine which propagation processes usually occur in nature and thus have to be represented by the model.

B. Scattering around BS and MS

The essential processes are line-of-sight (free space) propagation, single scattering around the MS or the BS, and double scattering (see Fig. 1).

The line-of-sight propagation is included inherently in any geometrical approach.

The single-scattering processes (BS→MS-scatterers→MS, and BS→BS-scatterers→MS) can be included by modeling the location of the scatterers around the BS and MS respectively, similar to the GSCM model of [7]. The scatterer locations determine both the DOA and the delay of the MPCs that propagate

via the near scatterers. Note that the distance of the scatterers (which determine the delays) must correspond to the physical MPCs that undergo *single* scattering. It must not be increased in order to accommodate delay dispersion that appears somewhere else in the propagation path[3] (i.e., in the mechanisms described in the next subsections). In addition to the scatterer distribution, we also have to define a "BS Rice factor" and a "MS Rice factor" to give the relative importance of BS→MS-scatterers→MS and BS→BS-scatterers→MS compared to the LOS propagation.[4]

The inclusion of the double-scattering process is more complicated. Existing models [9] assume that DOAs and DODs are separable, as waves can propagate from each BS-scatterer to each MS-scatterer with equal probability. This might be a good assumption in macrocells, but usually is not fulfilled in most microcellular and indoor environments with specular reflections. In that case, each scatterer near the BS will illuminate only very few scatterers near the MS - essentially with a certain angular spread that will depend on the surface roughness of the scatterers. It seems thus advantageous to define for each BS scatterer an angular distribution function including an angular spread that determines (together with the BS - MS distance) how many MS scatterers are illuminated by each BS scatterer (and vice versa). Note that this part of the model can account for some types of keyholes.

C. Scattering via far clusters

The next step is the inclusion of far clusters (see Fig. 2). This is especially relevant in outdoor environments. It usually requires an unobstructed view from the BS to the far scatterers, and from there to the MS. However, some scattering around the MS might still occur. Since it is single- or double scattering, we can treat the problem similar to the previous subsection. In other words, we first establish the location of the far scatterers in space, and assume that all of those are illuminated by the BS. Then, each far scatterer can illuminate the MS directly, or it can illuminate a certain (angular) range of MS scatterers. The required parameters (apart from the location of the far scatterers) are the "far scatterer Rice factor" (describing how much energy goes via a single-scattering process compared to the energy going via double-scattering processes), and the angular range that the far scatterers can illuminate. The delay dispersion can be increased by the presence of the far scatterers even within a cluster, since the possible variations of the runtime lengths increase. Also, since the number of clusters increases, the angular and delay dispersion both increase. Scattering that involves both BS-scatterers and far scatterers can usually be neglected, since it carries too little energy.

[3]Note that the placing of "equivalent" scatterers for single-scattering models that include delay dispersion incurred by other propagation effects is possible in single-directional models.

[4]Note that this is already the first important distinction from standard channel modeling, where only the normal Rice factor is considered, and can be extracted quite easily from measurements.

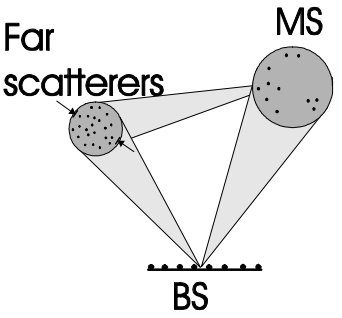

Fig. 2. Scattering via far clusters

D. Waveguiding and diffraction

The next, and rather difficult, step is the inclusion of waveguide propagation at some point between transmitter and receiver. It has been observed in several urban macro- and microcellular measurement campaigns [13], [14] that waves can be coupled into a street canyon (waveguide) either directly from the transmitter, or after reflection by near or far scatterers. Similarly, waves can propagate from TX or RX via a (horizontal) roof-edge directly or via other scatterers. These two propagation mechanisms (see Fig. 3) share a very important MIMO property as the associated propagation matrices are both rank-deficient [10]. However, there are also two differences:

1) the waveguide usually adds delay dispersion, while a roof-edge does not.
2) a horizontal roof-edge is rank-deficient (usually with rank one) with respect to vertical antenna arrangements, but does not restrict the rank with respect to horizontal arrangements. The waveguide is typically rank-deficient with rank higher than one in the horizontal dimension. The rank depends on the exact propagation circumstances. If there is pure waveguiding along a single street or a corridor, then the rank depends on the number of modes that the street (or a corridor) can support. If the waveguiding involves diffraction around one corner, then this would bring the rank (with respect to horizontal antenna arrangements) to unity. Note, however, that for a typical street crossing, all four corners neighboring the intersection are involved, which tends to increase the rank.

As a first approximation, we treat delay dispersion and rank deficiency in the waveguide in a multiplicative way. Although "waveguide dispersion" implies that different modes propagate with different speeds, which couples rank and delay dispersion, our preliminary simulations of frequency-selective MIMO channels have shown that this has negligible influence on the capacity distribution.

It is also important to note that waveguiding need not be implemented as a mutiple-diffraction process. Rather, random matrices multiplied by a "rank-reducing" matrix reproduce the statistical properties of the propagation in the waveguide; for

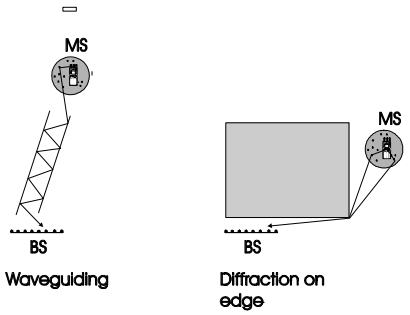

Fig. 3. Waveguiding and diffraction.

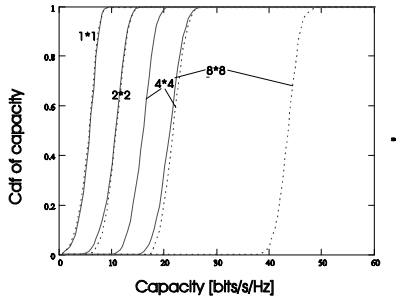

Fig. 4. Distribution of the capacity of a 1*1, 2*2, 4*4, and 8*8 system with our model and with idealized (independent Rayleigh fading) model.

details see [15].

III. Parameters values and simulation results

A. List of parameters

The above propagation effects can be described by parameterizing by the following features:

- scatterer around BS
- scatterer around MS
- N_c far scatterer clusters (each consisting of individual scatterer points)
- N_w waveguides and diffraction edges

A complete parametrization is given in Table 1. We note that this table does not include all large-scale variations of the impulse response. However, one benefit[5] of our cluster (or geometry) based approach is that large-scale variations of the clusters can be described in a much easier way. Specifically, most of the cluster properties derived in single-directional models (especially the COST259 model [3]) can be immediately reused, as they are identical for single- and double-directional models.

B. Generation of impulse responses and capacities

Once the parameters are known, impulse responses can be generated by simply adding up the contributions from the different propagation processes. The properties of the MPCs $h(\tau_i, \Omega_{R,i}, \Omega_{T,i})$ can be computed directly from the location of the scatterers; the entries of the matrix channel transfer function can be computed from Eq.(2) for different antenna configurations. With the knowledge of the transfer function matrix, we can now compute the capacity for both frequency-flat and frequency-selective channels. For the frequency-flat case, the capacity is given as

$$C = \log_2 \left[\det \left(I_{N_{\mathrm{r}} * N_{\mathrm{r}}} + \frac{\overline{\Gamma}}{N_{\mathrm{t}}} \underline{H} \underline{H}^H \right) \right]$$

where $I_{N_{\mathrm{r}} * N_{\mathrm{r}}}$ is the $N_{\mathrm{r}} * N_{\mathrm{r}}$ identity matrix and $\overline{\Gamma}$ is the mean signal-to-noise ratio (SNR) per receiver branch, and $\underline{H}$ contains the transfer functions from $x_{R,m}$ to $x_{T,k}$.

[5] in addition to those mentioned in Sec. II

For the frequency-selective case, it is best to transform the impulse responses into the frequency domain, to obtain the normalized capacity as

$$C = \frac{1}{B} \int_B \log_2 \left[\det \left(I_{N_{\mathrm{r}} * N_{\mathrm{r}}} + \frac{\overline{\Gamma}}{N_{\mathrm{t}}} \underline{H}(f) \underline{H}(f)^H \right) \right] df \quad (5)$$

where B is the considered bandwidth. In either case, the capacity is a random variable, since the transfer function matrix entries are random variables [2].

C. Results

Figure 4 shows the outage capacity distribution for a channel with parameters that are typical in an urban macrocell with a large distance between BS and MS (with the parameters given in the third column of Table 1). Results are shown for single-antenna systems $(1 * 1)$ as well as $2 * 2$, $4 * 4$, and $8 * 8$ systems. For comparison, we also show results for the "ideal" case, namely independent Rayleigh fading on all antenna elements. We see that for a small number of antennas, the achievable realistic capacities are very close to the ideal ones. However, as the number of antenna elements increases, the difference between ideal and realistic case becomes more pronounced. This can be explained by the fact that there are several "rank-reduced" contributions in the total channel matrix, so that additional antenna elements do not have enough independent transmission paths to support independent data streams. Note that the "ideal" model gives lower capacity than our model in the $1 * 1$ case. This is due to the fact that our model includes a LOS component, which decreases the probability of deep fades.

Note also that the difference between our computed capacities and the idealized capacities is on the order of 30% for a $4*4$ system, lies between the measurement results of [16] and [17]. While this is not a proof for the validity of our parametrization,[6] it is at least a satisfactory "sanity check".

[6] Neither of those two experiments had a setup that corresponded completely with our setup for Fig. 2. The measurements of Xu et al. had a very strong LOS component, while the measurements of Martin et al. used antennas that were spaced much farther apart. I also performed simulations for those specific setups, and got good agreement with the measurement results.

IV. Summary and conclusion

We have presented a generic model for MIMO wireless channels. We identified the most important propagation mechanisms, and established a physical model. It takes into account the scattering near BS and MS, as well as scattering by far clusters, multiple scattering, diffraction, and waveguiding effects. Also, the fact that there is only a limited number of scatterers is taken into account. All these effects contribute to eigenvalue distributions that are different from those of an independent Rayleigh-fading channel, and thus imply a lower capacity. Some exemplary capacity distribution curves, based on typical parameter choices, exemplified those capacity losses. We also gave equations for the impulse responses as a function of the parameters, both in the double-directional formulation, and the matrix channel formulation that can be used to characterize MIMO channels.

The complete characterization of the model requires a considerable number of parameters. A full establishment of all statistical distribution of these parameters is a daunting task, and will keep experimentalists busy for many years to come. Still, we think that this is the first time that a complete generic MIMO channel model has been presented, and only on this basis can a comprehensive measurement program be performed and evaluated. Furthermore, the formulation of the model also allows reuse of many of the insights and data gained in previous single-directional or non-directional measurement campaigns.

Acknowledgements: The author would like to thank Dr. Jack Winters and Dr. Larry Greenstein for critical reading of the manuscript and helpful suggestions.

References

[1] J. H. Winters, "On the capacity of radio communications systems with diversity in Rayleigh fading environments," *IEEE J. Selected Areas Comm.*, 1987.

[2] G. J. Foschini and M. J. Gans, "On limits of wireless communications in a fading environment when using multiple antennas," *Wireless Personal Communications*, vol. 6, pp. 311–335, 1998.

[3] M. Steinbauer and A. F. Molisch, *Directional Channel Modelling*, ch. 3.2, pp. 148–194. Wiley, 2001.

[4] D. Shiu, G. Foschini, M. .Gans, and J. Kahn, "Fading correlation and its effect on the capacity of multi-element antenna systems," *IEEE Trans. Comm.*, vol. 48, pp. 502–513, 2000.

[5] W. C. Jakes, *Microwave Mobile Communications*. IEEE Press, 1974.

[6] W. C. Y. Lee, "Effects on correlation between two mobile radio base-station antennas," *IEEE Trans. Comm.*, vol. 21, pp. 1214–1224, 1973.

[7] J. Fuhl, A. Molisch, and E. Bonek, "Unified channel model for mobile radio systems with smart antennas," *IEE Proc. Radar, Sonar and Navigation*, vol. vol. 145, no. 1, pp. 32–41, 1998.

[8] H. Boelcskei, D. Gesbert, and A. Paulraj, "On the capacity of wireless systems employing OFDM-based spatial multiplexing," *IEEE Trans. Comm.*, p. submitted, 2000.

[9] D. Gesbert, H. Bolcskei, D. Gore, and A. J. Paulraj, "MIMO wireless channels: Capacity and performance prediction," in *Proc. Globecomm 2000*, (San Francisco), pp. 1083–1088, IEEE, 2000.

[10] D. Chizhik, G. J. Foschini, and R. A. Valenzuela, "Capacities of multi-element transmit and receive antennas: Correlations and keyholes," *Electronics Lett.*, vol. 36, pp. 1099 –1100, 2000.

[11] T. Svantesson, *Antennas and Propagation from a Signal Processing Perspective*. PhD thesis, Chalmers University, Sweden, 2001.

[12] M. Steinbauer, A. F. Molisch, and E. Bonek, "The double-directional mobile radio channel," *IEEE Antennas and Propagation Mag.*, p. in press, 2000.

[13] M. Toeltsch, J. Laurila, A. F. Molisch, K. Kalliola, P. Vainikainen, and E. Bonek, "Spatial characterization of urban mobile radio channels," in *Proc. VTC2001 Spring*, (Rhodes, Greece), IEEE, 2001.

[14] A. Kuchar, J. P. Rossi, and E. Bonek, "Directional macro-cell channel characterization from urban measurements," *IEEE Trans. Antennas Prop.*, vol. 48, pp. 137 –146, 2000.

[15] A. F. Molisch, "A generic model for MIMO wireless propagation channels," *IEEE Trans. Comm.*, to be submitted.

[16] C. C. Martin, J. H. Winters, and N. R. Sollenberger, "Multiple-input multiple-output (MIMO) radio channel measurements.," in *Proc. VTC Fall 2000*, (Boston), 2000.

[17] H. Xu, M. J. Gans, M. Amitay, and R. A. Valenzuela, "Experimentla verification of MTMR system capacity in cotrolled propagation environment.," *Electronics Lett.*, vol. 37, pp. 936–937, 2001.

variable	meaning	Typical value in urban macrocell
$P_{NB\text{-}NLOS}$	Narrowband power carried by non-LOS contributions	Chosen to agree with Okomura-Hata
K_{Rice}	Rice factor	-10dB
$N_{BSscatt}$	Number of scatterers around BS	4
$pdf_{BS}(r,\varphi, z)$	Distribution of scatterers around BS	$\frac{1}{10}\exp(-r^2/2\cdot 100^2)$ for $-5<z<5$
$P_{Bsscatt}$	Power carried by BS scatterers if all are illuminated uniformly by a source at the MS (relative to $P_{NB\text{-}NLOS}$)	$-\infty dB$
$N_{Msscatt}$	Number of scatterers around MS	12
$pdf_{MS}(r,\varphi, z)$	Distribution of scatterers around MS	$\frac{1}{15}\exp(-r^2/2\cdot 100^2)$ for $-5<z<10$
$P_{Msscatt}$	Power carried by MS scatterers if all are illuminated uniformly by a source at the BS (relative to $P_{NB\text{-}NLOS}$)	-2.2dB
$P_{doublescatt}$	power carried by MPCs that are scattered by scatterers both near the MS and BS	$-\infty dB$
$\varphi_{mean,illum}$	Mean of the illumination angle of scatterers at MS by scatterers at BS and vice versa	Uniform in seen region
$\varphi_{spread,illum}$	Spread of the illumination angle of scatterers at MS by scatterers at BS and vice versa	2 degrees
N_{fc}	Number of far clusters	1
N_w	Number of waveguides and edges	*3* (one roofedge, 2 waveguides)
For each far cluster		
$N_{fcscatt}$	Number of scatterers in the far cluster	10
$pdf_{fc}(r,\varphi)$	Distribution of scatterers in the far cluster	$\exp(-(r-r_0)^2/2\cdot 100^2)$ location of cluster centers uniform in cell
P_{fc}	power carried by the far cluster (relative to $P_{NB\text{-}NLOS}$)	-10dB
$P_{fc\text{-}Bsscatt}$	Power carried by MPCs that go via BS-scatterer (relative to P_{fc})	$-\infty dB$
$P_{fc\text{-}Msscatt}$	power carried by MPCs that go via MS-scatterer (relative to P_{fc})	-7dB
$\varphi_{spread,illum,fcBS}$	Spread of the illumination angle of scatterers at BS by far scatterers and vice versa	All scatterers illuminated
$\varphi_{spread,illum,fcBS}$	Spread of the illumination angle of scatterers at MS by far scatterers and vice versa	All scatterers illuminated
For each waveguide or edge		
P_w	power carried by waveguide (relative to $P_{NB\text{-}NLOS}$)	-10dB
$h(\tau)$	additional time dispersion created in the waveguide	$\exp(-\tau/\upsilon)$ ν=200ns (waveguide), 0ns (edge)
$pdf(\lambda_{i,v})$	Eigenvalue distribution of the propagation matrix for horizontal components	$\exp(-\lambda/4)$
$pdf(\lambda_{i,h})$	Eigenvalue distribution of the propagation matrix for vertical components	$\exp(-\lambda/0.01)$
$P_{w,Bsdirect}$	Power coupled into the waveguide directly (relative to P_w)	-0.45dB
$P_{w,Bsscatt}$	Power coupled into waveguide via BS scatterers (relative to P_w)	$-\infty dB$
$\varphi_{spread,illum,wBS}$	Angular spread of the BS scatterers that couple power into the waveguide	All scatterers illuminated
$P_{w,Msdirect}$	Power is coupled out of the waveguide directly (relative to P_w)	-6dB
$P_{w,Msscatt}$	Power coupled into the waveguide via MS scatterers (relative to P_w)	-6dB
$\varphi_{spread,illum,wBS}$	Angular spread of the MS scatterers that couple power into the waveguide	All scatterers illuminated
$P_{w,fc\text{-}BS}$	Power coupled into to the waveguide by each of the far scatterer clusters	-10dB

Fig. 5. Table 1: List of parameters for the description of the MIMO model.